An Improved Control Law Using HVDC Systems for Frequency Control

Jing Dai, G. Damm

An improved control law using HVDC systems for frequency control

Jing Dai and Gilney Damm

***Abstract*—**

I. Introduction

Traditionally, among all the converters of a multi-terminal HVDC system, only one keeps the power balance of the DC grid by regulating its DC voltage (slack bus), while all the others transfer a pre-scheduled amount of power. This operation mode is very simple to implement, and it can prevent cascade outage. However, it also has some drawbacks: (i) the zone of the converter regulating the DC voltage must be strong enough to counteract the disturbance resulting from the disconnection of other zones. This is especially pronounced in the case of a multi-terminal HVDC system that connects several zones of relatively similar sizes; (ii) the primary frequency control reserves are not shared among the zones, i.e. when one zone suffers from a power imbalance resulting in a frequency excursion, other zones would not respond to help rebuild its power balance, as the case in an AC interconnection.

To address the first disadvantage, some articles (e.g. [2]) generalized the notion of decentralized slack bus to HVDC systems, where more than one converter are used to regulate the DC voltage. For the second disadvantage, some articles (e.g. [1], [4], [5], [6], [7]) proposed control law to share primary reserves among the zones. Most of these control laws change the power transferred through the converters based on remote frequency information, where the delays associated with the indispensable communication between remote zones may jeopardize stability [3]. To free from this dependence on remote information, Reference [4] proposed a control scheme where each converter controls its DC voltage such that its deviation is proportional to the local frequency deviation. This control scheme implicitly requires that all the converters are slack buses, which simultaneously addresses the first drawback. The use of only local information gives the control scheme an advantage of being decentralized. However, as no communication between the zones is involved, the frequency deviations of the areas would remain different in steady state following a power imbalance. It is true that such differences can be made smaller by increasing the controller gain, but a large controller gain would also jeopardize system stability. Moreover, these steady-state differences also imply a smaller degree of reserves sharing, compared with the case of a sheer AC interconnection.

J. Dai and G. Damm are with Laboratoire des Signaux et Systèmes (LSS), Supélec, 3 rue Joliot-Curie, 91192 Gif-sur-Yvette, France jing.dai@supelec.fr, gilney.damm@lss.supelec.fr

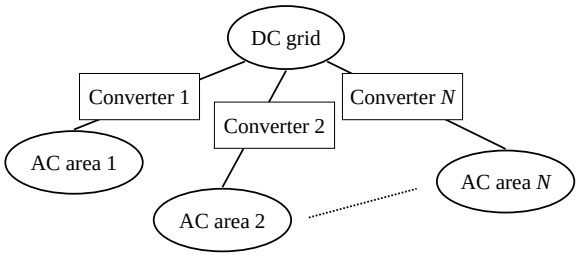

Fig. 1. A multi-terminal HVDC system connecting N AC areas via N converters.

This article proposes an improved version of the control law proposed in [4]. By including an integral term of the local frequency deviation, the new control scheme is able to eliminate the differences between the zones' frequency deviations. However, as the integral term has a cumulative effect on the DC voltage, another term necessitating communication between the converters is also introduced, which aims at preventing the DC voltage from drifting away. Fortunately, the required communication needs not to be instantaneous, and this term with remote information can be updated at a slower rate without compromising the control law's ability on reserve sharing.

The rest of the paper is organized as follows. Section II models the HVDC system and defines a reference operating point. Section III elaborates on the new control law and theoretically proves its stability. Section IV gives simulation results and discusses the practical implementation of the control law. Section V concludes.

II. Multi-terminal HVDC system model and reference operating point

A. System model

The multi-terminal HVDC system model considered in this paper is composed of a DC grid, N separate AC areas, and N converters that interface the AC areas with the DC grid, as shown in Figure 1.

The dynamics of each AC area are modeled as

$$2\pi J_i \frac{df_i}{dt} = \frac{P_{mi} - P_{li} - P_i^{dc}}{2\pi f_i} - 2\pi D_{gi}(f_i - f_{nom,i}), \tag{1}$$

$$T_{smi} \frac{dP_{mi}}{dt} = P_{mi}^o - P_{mi} - \frac{P_{nom,i}}{\sigma_i} \frac{f_i - f_{nom,i}}{f_{nom,i}}, \tag{2}$$

$$P_{li} = P_{li}^o \cdot (1 + D_{li}(f_i - f_{nom,i})), \tag{3}$$

where the state variables are f_i, the frequency of area i (which can be readily measured), and P_{mi}, the mechanical

power input in the areas. Other variables in the above equations are P_{li}, the aggregated load of area i, and P_i^{dc}, the power injected from area i into the DC grid. The parameters are: $f_{nom,i}$ the nominal frequency, P_{li}^o the aggregated load of area i at the nominal frequency, D_{li} frequency sensitivity factor of the aggregated load, J_i the moment of inertia of the aggregated generator of area i, D_{gi} the damping factor of the generator, σ the generator droop, P_{nom} the rated mechanical power of the generator, P_m^o the reference value of P_{mi} at the nominal frequency, and T_{sm} the time constant associated with the dynamics of primary frequency control. Briefly speaking, Equation (1) describes how the frequency varies as a result of the power balance within area i, (2) characterizes primary frequency control that adjusts the generator's mechanical power in response to frequency excursions, and (3) shows the frequency-dependent nature of the load. Detailed physical interpretation of the above equations can be found in [5].

The DC grid interconnects the AC areas via the converters. By Ohm's law, the power P_i^{dc} satisfies

$$P_i^{dc} = \sum_{k=1}^{N} \frac{V_i^{dc}(V_i^{dc} - V_k^{dc})}{R_{ik}} \ , \tag{4}$$

where V_i^{dc} and V_k^{dc} are the DC voltages of converters i and k respectively and R_{ik} is the effective resistance between these two points in the DC grid. Each converter is considered to be capable of instantaneously applying a control input in the form of either the power injection P_i^{dc} or the DC voltage V_i^{dc}. In other words, either P_i^{dc} or V_i^{dc} can be used as the control variable.

B. Reference operating point

The reference operating point of the system is a steady state at which the system is supposed to rest prior to any disturbance. It is defined by specific values of the input parameters (P_{li}^o, P_{mi}^o) and the variables (f_i, P_{mi}, P_{li}, P_i^{dc}, V_i^{dc}). We denote values at the reference operating point by the corresponding symbols with a bar overhead.

At the reference operating point, for $i = 1, 2, ..., N$, $\bar{f}_i = f_{nom,i}$. Then (3) directly yields $\bar{P}_{li} = \bar{P}_{li}^o$, and imposing equilibrium in (2) yields $\bar{P}_{mi} = \bar{P}_{mi}^o$ and in (1) yields $\bar{P}_i^{dc} = \bar{P}_{mi}^o - \bar{P}_{li}^o$. Equation (4) provides a final set of equations linking the voltage values to the other variables $\bar{P}_i^{dc} = \sum_{k=1}^{N} \bar{V}_i^{dc}(\bar{V}_i^{dc} - \bar{V}_k^{dc})/R_{ik}$.

III. Control law

A. Original control law

The original control law proposed in [4] is

$$\Delta V_i^{dc} = \alpha \Delta f_i \ , \tag{5}$$

where $\Delta V_i^{dc} = V_i^{dc} - \bar{V}_i^{dc}$ and $\Delta f_i = f_i - \bar{f}_i$. In response to a power imbalance in one area, this control law makes the Δf_i close to each other, but the differences between them can not be eliminated, which leads to a smaller degree of primary frequency control reserve sharing compared to the case with the control law studied in [3], [5] that results in identical Δf_i in all zones.

B. Improved control law

To eliminate the differences between Δf_i in steady state, we propose the following improved control law:

$$\frac{d\Delta V_i^{dc}}{dt} = \alpha \frac{d\Delta f_i}{dt} + \beta \Delta f_i - \gamma \sum_{k=1}^{N} \Delta V_k^{dc} \ . \tag{6}$$

Compared to (5), the new control law includes two additional terms. The integral term of Δf_i is used to nullify the differences between f_i, while the integral term of the sum of ΔV_i^{dc} of all the zones aims at preventing the continual drifting of V_i^{dc}. In fact, if $\gamma = 0$, then, even when all Δf_i have already converged to a (common) steady-state value, ΔV_i^{dc} would still keep drifting away as long as $\Delta f_i = 0$. On a larger time scale, when f_i is restored to f_{nom} thanks to the secondary frequency control, the new steady state value of V_i^{dc} would be different from its value prior to the disturbance[1], implying a continual change of working point of the converters as power imbalances occur in the areas.

The introduction of the γ term in the control law (6) makes it no longer decentralized. However, as will be shown in Section IV-C, the communication does not have to be instantaneous, and the γ term be updated at a slower rate without compromising the control law's effectiveness.

C. Theoretical study

In this part, we study the stability property of the closed-loop system linearized around the reference operating point as follows. Equation (1) is linearized with (3) taken into consideration as

$$2\pi J_i \frac{df_i}{dt} = \frac{P_{mi} - P_{li}^o - P_i^{dc}}{2\pi f_i} - 2\pi D_i(f_i - f_{nom,i}) \tag{7}$$

where $D_i = D_{gi} + \bar{P}_{li}^o D_{li}/(4\pi^2 f_{nom,i})$. The DC load flow equation (4) is linearized as

$$P_i^{dc} = \frac{\bar{P}_i^{dc}}{\bar{V}_i^{dc}} V_i^{dc} + \sum_{k=1}^{N} \frac{\bar{V}_i^{dc}}{R_{ik}} (V_i^{dc} - V_k^{dc}) \ . \tag{8}$$

Proposition 1: Consider the linearized system (2), (7), (8) under the control law (6). Then at the equilibrium point associated to load imbalances, the frequency deviations of all areas are equal.

Proof: At equilibrium, the differential equation (6) with time derivatives equal to zero yields

$$\Delta f_i = \frac{\gamma}{\beta} \sum_k \Delta V_k^{dc} \ . \tag{9}$$

As the expression of Δf_i is independent of the area index i, the frequency deviations of all areas are identical. □

Proposition 2: Consider the closed-loop system (2), (6), (7), (8). Then at the equilibrium point associated to load

[1]It is true that positive and negative power imbalances may eventually cancel each other's cumulative effects on the drifting of V^{dc}. However, this shift of operating point in V^{dc} may become unacceptable in the long term when either positive or negative imbalances happen to occur and their cumulative effects make the converters' DC voltage drift to an unacceptably high or low value.

imbalances, the system is stable and converges to its equilibrium point.

Proof: Let $x_i = \Delta f_i$, $y_i = P_{mi} - \bar{P}_{mi}$, $u_i = P_i^{dc} - \bar{P}_i^{dc}$, $v_i = \Delta V_i^{dc}$, $d_i = P_{li}^o - \bar{P}_{li}^o$. Define the vectors $\mathbf{x} = [x_1, x_2, \ldots, x_N]^T$, $\mathbf{y} = [y_1, y_2, \ldots, y_N]^T$, $\mathbf{u} = [u_1, u_2, \ldots, u_N]^T$, $\mathbf{v} = [v_1, v_2, \ldots, v_N]^T$, $\mathbf{d} = [d_1, d_2, \ldots, d_N]^T$. Then, Equations (2), (6), (7), (8) can be written in matrix form representing the entire interconnected system as

$$\frac{d\mathbf{x}}{dt} = -A_1\mathbf{x} + A_2\mathbf{y} - A_2\mathbf{u} - A_2\mathbf{d} \,, \tag{10}$$

$$\frac{d\mathbf{y}}{dt} = -A_3\mathbf{x} - A_4\mathbf{y} \,, \tag{11}$$

$$\frac{d\mathbf{v}}{dt} = \alpha\frac{d\mathbf{x}}{dt} + \beta x + \gamma 1_N^T\mathbf{v}1_N \,, \tag{12}$$

$$\mathbf{u} = (\bar{C} + \bar{V}L)\mathbf{v} \,, \tag{13}$$

where $A_1 = \text{diag}\{D_i/J_i\}$, $A_2 = \text{diag}\{1/(4\pi^2 f_{nom,i}J_i)\}$, $A_3 = \text{diag}\{P_{nom,i}/(T_{smi}\sigma_i f_{nom,i})\}$, $A_4 = \text{diag}\{1/T_{smi}\}$, $\bar{C} = \text{diag}\{\bar{P}_i^{dc}/\bar{V}_i^{dc}\}$, $\bar{V} = \text{diag}\{\bar{V}_i^{dc}\}$, and 1_N is the column vector of length N with all elements equal to 1.

Replacing $d\mathbf{x}/dt$ in (12) by (10) yields

$$\begin{aligned}\frac{d\mathbf{v}}{dt} =& (-\alpha A_1 + \beta I_N)\mathbf{x} + \alpha A_2\mathbf{y} \\ & - \alpha A_2\mathbf{u} - \alpha A_2\mathbf{d} - \gamma 1_N^T\mathbf{v}1_N \,,\end{aligned} \tag{14}$$

where I_N is the identity matrix of dimension N and we used the fact that $1_N^T\mathbf{v}1_N = 1_N 1_N^T\mathbf{v}$. By eliminating $\mathbf{u}$, we can write the closed-loop system as

$$\frac{d}{dt}\begin{pmatrix}\mathbf{x}\\ \mathbf{y}\\ \mathbf{v}\end{pmatrix} = S\begin{pmatrix}\mathbf{x}\\ \mathbf{y}\\ \mathbf{v}\end{pmatrix} + \begin{pmatrix}A_2\\ 0\\ 0\end{pmatrix}\mathbf{d} \,, \tag{15}$$

where

$$S = \begin{pmatrix} -A_1 & A_2 & -A_2(\bar{C} + \bar{V}L) \\ -A_3 & -A_4 & 0 \\ -\alpha A_1 + \beta I & \alpha A_2 & -\alpha A_2(\bar{C} + \bar{V}L) - \gamma 1_N 1_N^T \end{pmatrix} .$$

Through some rank-preserving transformations, it can be shown that S is full ranked. Thus, the steady-state values of $\mathbf{x}$, $\mathbf{y}$ and $\mathbf{v}$ are unique and are given by

$$\begin{pmatrix}\mathbf{x}_{ss}\\ \mathbf{y}_{ss}\\ \mathbf{v}_{ss}\end{pmatrix} = S^{-1}\begin{pmatrix}A_2\mathbf{d}\\ 0\\ 0\end{pmatrix} \,. \tag{16}$$

In the following, we prove by contradiction that all the eigenvalues of S must have negative real part. Denote by $\Re e(\cdot)$ the real part of a complex number. Suppose that S has an eigenvalue λ such that $\Re e(\lambda) > 0$. Let $(q_1, q_2, q_3)^T$ be its corresponding eigenvector, then we can find

$$(\bar{C} + \bar{V}L)q_3 = -A^* q_1 \,, \tag{17}$$

$$(\lambda I_N + \gamma 1_N 1_N^T)q_3 = (\alpha\lambda + \beta)q_1 \,, \tag{18}$$

where

$$A^* = \left(\frac{A_1 + \lambda I_N}{A_2} + \frac{A_3}{A_4 + \lambda I_N}\right) .$$

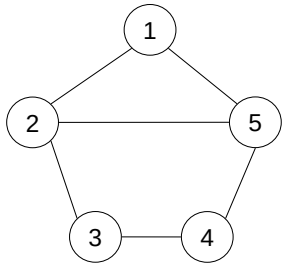

Fig. 2. Topology of the DC grid.

TABLE I

PARAMETERS AND INITIAL VALUES FOR THE AC AREAS.

AC area	1	2	3	4	5	Unit
P_{nom}	50	80	50	30	80.4	MW
J	2026	6485	6078	2432	4863	kg m^2
D_g	48.4	146.4	140	54.7	95.1	W s^2
σ	0.02	0.04	0.06	0.04	0.03	/
T_{sm}	1.5	2.0	2.5	2	1.8	s
P_l^o	100	60	40	50	40	MW
$\bar{P}^{dc}$	-50	20	10	-20	40.4	MW
$\bar{V}^{dc}$	99.17	99.60	99.73	99.59	100	kV
$f_{nom,i} = 50$Hz, $D_{li} = 0.01$s, and $P_{m,i}^o = P_{nom,i}$ for all i.						

Let $q_r = \bar{V}^{-1}A^*q_1$. Then, the above equations are equivalent to

$$q_r = -(\bar{C}\bar{V}^{-1} + L)q_3 \,, \tag{19}$$

$$q_r = (\alpha\lambda + \beta)^{-1}\bar{V}^{-1}A^*(\lambda I_N + \gamma 1_N 1_N^T)q_3 \,. \tag{20}$$

Since $\Re e(\lambda) > 0$, Equation (19) requires $\Re e(q_3^* q_r) < 0$ while (19) requires[2] $\Re e(q_3^* q_r) > 0$, which are contradictory. Therefore, such a λ with positive real part cannot exist, and the closed-loop system is thus stable, and, following a power imbalance, it converges to the unique equilibrium point given by (16). □

IV. SIMULATION RESULTS AND PRACTICAL IMPLEMENTATION

A. Simulated system

To empirically test the new control law, we run simulations on the same system as used in [3], [4], [5]. The system is composed of five AC areas, interconnected by a DC grid whose topology is shown in Figure 2. The parameters of the AC areas are shown in Table I, where the resistances of the DC grid are: $R_{12} = 1.39\Omega$, $R_{15} = 4.17\Omega$, $R_{23} = 2.78\Omega$, $R_{25} = 6.95\Omega$, $R_{34} = 2.78\Omega$ and $R_{45} = 2.78\Omega$. The full nonlinear system model (1), (2), (3), (4) is simulated using an Euler method with a time-discretization step of 1ms. The load disturbance considered is a step increase by 2% of P_{l2}^o.

[2]The matrix $1_N 1_N^T$ is positive definite, because

$$x^T 1_N 1_N^T x = (x^T 1_N)(1_N^T x) = (1_N^T x)^2 \,.$$

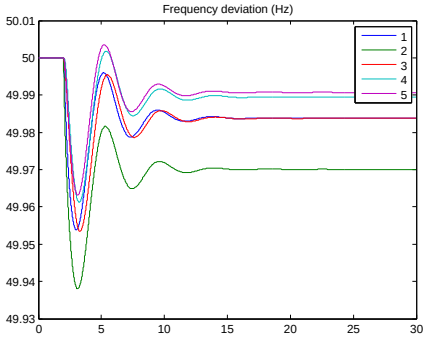

Fig. 3. f_i under the original control law (5).

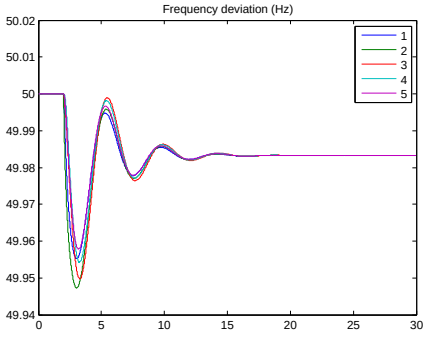

Fig. 4. f_i under the new control law (6).

B. Simulation results

The frequencies of the AC areas under the original control law (5) and the new one (6) are shown respectively in Figures 3 and 4. These figures show that the new control law eliminates the steady-state differences between the frequency deviations. The control variables (V^{dc}) under the new control law with $\gamma = 0.1$ and $\gamma = 0$ are shown respectively in Figures 5 and 6, which demonstrate the role of the γ term in (6) of preventing the continuous drifting of V_i^{dc}.

C. Practical implementation

The introduction of the γ term necessitates communication between the HVDC terminals. To take into account the delay, the γ term are updated only every 500 ms. The resulting curves of f_i and V_i^{dc} are shown respectively in Figures 7 and 8. Compared to Figures 4 and 5, the less frequent update of the γ term seems to have little impact on f_i, but it render the curves of V_i^{dc} serrated, which would pose no problem to the operation of HVDC converters.

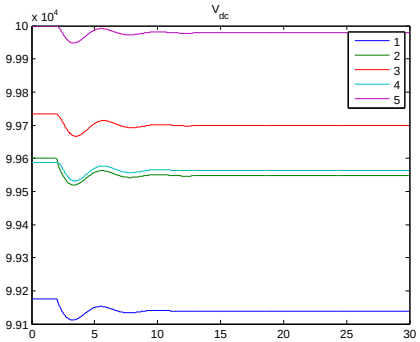

Fig. 5. V_i^{dc} under the new control law (6) when $\gamma = 0.1$.

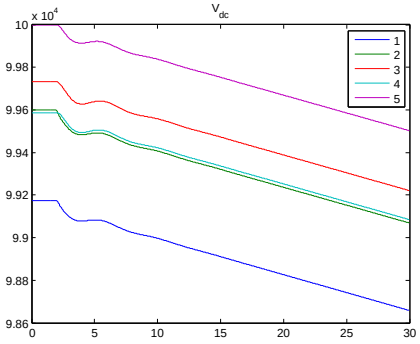

Fig. 6. V_i^{dc} under the new control law (6) when $\gamma = 0$.

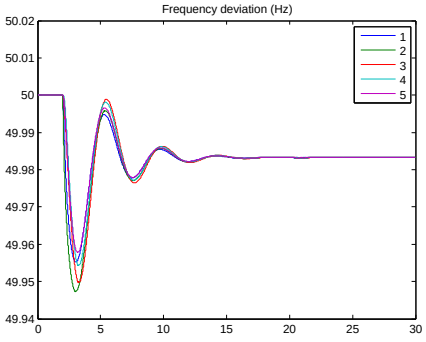

Fig. 7. f_i under the new control law (6) when the γ term is updated every 500ms.

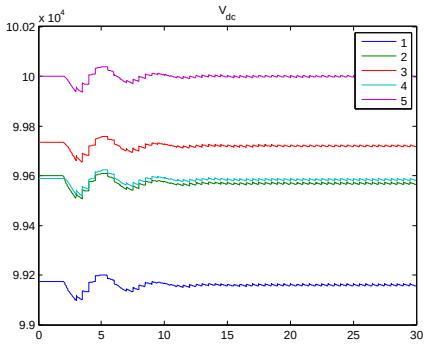

Fig. 8. V_i^{dc} under the new control law (6) when the γ term is updated every 500ms.

V. Conclusions

This paper proposed an improve version of a control law originally proposed in [4] that modifies the DC voltages of the HVDC converters in order to share the primary frequency control reserves between the AC areas connected by the HVDC grid. Compared to the original control law, the new one is able to eliminate the differences between the AC areas' frequencies in steady state, which results in a higher degree of reserve sharing. A theoretical study proved the stability of the linearized system under the new control law, and simulation results on the nonlinear system demonstrate its effectiveness.

References

[1] B. H. . Bakken and H. H. Faanes, "Technical and economic aspects of using a long submarine HVDC connection for frequency control", *in IEEE Transactions on Power Systems*, vol. 12, pp. 1252-1258, August 1997.

[2] J. Beerten, D. Van Hertem and R. Belmans, "VSC MTDC systems with a distributed DC voltage control - A power flow approach", *in Proceedings of 2011 IEEE Trondheim PowerTech*, Trondheim, Norway, 19-23 June 2011, 6 pages.

[3] J. Dai, Y. Phulpin, A. Sarlette and D. Ernst, "Impact of delays on a consensus-based primary frequency control scheme for AC systems connected by a multi-terminal HVDC grid", *in Proceedings of the 2010 IREP Symposium - Bulk Power Systems Dynamics and Control - VIII*, Buzios, Rio de Janeiro, Brazil, 1-6 August 2010, 9 pages.

[4] J. Dai, Y. Phulpin, A. Sarlette and D. Ernst, "Voltage control in an HVDC system to share primary frequency reserves between non-synchronous areas", *in Proceedings of the 17th Power Systems Computation Conference (PSCC 2011)*, Stockholm, Sweden, August 22-26, 2011, 8 pages.

[5] J. Dai, Y. Phulpin, A. Sarlette and D. Ernst, "Coordinated primary frequency control among nonsynchronous systems connected by a multi-terminal HVDC grid", *IET Generation, Transmission & Distribution*, February 2012, Volume 6, Issue 2, pp. 99-108.

[6] T. M. Haileselassie, R. E. Torres-Olguin, T. K. Vrana, K. Uhlen, and T. Undeland, "Main grid frequency support strategy for VSC-HVDC connected wind farms with variable speed wind turbines", *in Proceedings of the 2011 PowerTech*, Trondheim, Norway, June 2011.

[7] M. Sanpei, A. Kakehi, and H. Takeda, "Application of multi-variable control for automatic frequency controller of HVDC transmission system", *IEEE Transactions on Power Delivery*, vol. 2, pp. 1063-1068, April 1994.